

# Revealing the presence of creatine in human spinal cord in amyotrophic lateral sclerosis, by infrared microspectroscopy

Magdalena Szczerbowska-Boruchowska,<sup>a\*</sup> Joanna Chwiej,<sup>a</sup> Paul Dumas,<sup>b</sup> Barbara Tomik<sup>c</sup> Dariusz Adamek<sup>c</sup> and Marek Lankosz<sup>a</sup>

<sup>a</sup>Faculty of Physics and Applied Computer Science, AGH University of Science and Technology, Krakow, Poland. E-mail: boruchowska@novell.ftj.agh.edu.pl

<sup>b</sup>SOLEIL Synchrotron, L'Orme des Merisiers, BP 48, F-91192 GIF-sur-Yvette Cedex, France

<sup>c</sup>Institute of Neurology, Jagiellonian University, Medical College, Krakow, Poland

## Introduction

Amyotrophic Lateral Sclerosis (ALS) is a fatal, progressive, neurodegenerative disorder. It occurs both sporadically and in about 10–15% of cases as a familial disease.<sup>1</sup> The main hallmark of ALS is the loss of motor neurons from selected areas of central nervous system tissue (ventral horns of spinal cord, cortex and brainstem) and its symptoms are associated with the progressive weakness and atrophy of skeletal muscles. However, the etiology of the disease remains unknown. Although, there is a group of interplaying processes that are suspected to lead to the atrophy and death of nerve cells in the case of ALS. These are: oxidative stress, mitochondrial dysfunction, excitotoxicity and protein aggregation. Moreover, mutations in the gene encoding Cu/Zn-superoxide dismutase are observed in 10–25% of familial cases of ALS.<sup>1</sup> Although the group of patients suffering from ALS varies with reference to symptoms, progress, duration of the disease etc., the sporadic and familial cases of the disorder are indistinguishable based on their clinical and pathological features. Because of this, it is expected that the mechanisms of pathogenesis

are the same in sporadically occurring and familial cases of ALS.

We have previously investigated the topographic and quantitative changes in the distribution of trace metals in spinal cords from ALS and control patients.<sup>2</sup> X-ray fluorescence microscopy was used to investigate their metallic nature and distribution in single nerve cells. A deeper understanding of the neurodegenerative processes in ALS requires focus on the biochemical changes occurring in nervous tissue of such a disorder. For this purpose, we have undertaken an infrared microspectroscopy study. While metals are suggested to play a pivotal role in the pathogenesis of ALS, they typically do not occur in tissues as free ions. This results in the presence of the complex mechanisms of metal ions buffering that protect cells against their toxic effects. Metal homeostasis is regulated by several proteins. Such proteins containing metal cofactor are called metalloproteins.<sup>1</sup>

Additionally, metallic traces may induce protein aggregation that is the common hallmark of many neurodegenerative disorders, such as Alzheimer's disease, Parkinson's disease, amyotrophic lateral sclerosis and prion diseases.<sup>3</sup> The plaques and tangles observed in

Alzheimer's disease are composed of Amyloid-beta and tau protein, respectively. Alpha-synuclein is the protein closely related to Parkinson's disease and the main component of characteristic for this disorder: Lewy bodies. Cytoplasmatic inclusions of different type (Bunina bodies, hyaline "balls", Lewy body-like and skein-like inclusions) are observed in ALS motor neurons as well. As was mentioned above, different protein aggregates were found in the case of ALS. However, none of them is typical for (or correlated with) the form of the disorder or the stage of the disease.<sup>4</sup> Although the above-mentioned neurodegenerative disorders are associated with different protein(s), the fibrils show, in the different pathologies, similarities in respect of their structural features.<sup>5</sup> Typically, the filaments have the molecular fine structure of amyloid. The amyloid-like fibrils with a diameter of around 10 nm demonstrate cross-beta structure and characteristic dye-binding properties.<sup>6</sup>

The organic composition of tissues and cells can be satisfactorily determined with the use of Fourier transform infrared (FT-IR) microspectroscopy. This technique combines IR spectroscopy and microscopy, enabling the determination of the

biochemical composition in small sample areas. Infrared spectroscopy can identify specific molecular functional groups associated with specific organic materials.<sup>7</sup> FT-IR microspectroscopy is a unique resource to provide a global analysis of the organic content of biological samples (proteins, lipids, carbohydrates, nucleic acids).<sup>8</sup> Regarding ALS studies, information gathered by the FT-IR technique can address the role of oxidative stress and apoptosis in ALS, mitochondrial dysfunction, increased peroxidation of lipids, changes in the activity of enzymes of the antioxidant system. Especially important with respect to neurodegenerative disorders and to ALS, is that FT-IR spectroscopy can provide unique information on molecular structure, mainly for determining the secondary structure of proteins.<sup>9</sup> The FT-IR microspectroscopy technique is providing new insights into the understanding of biochemical mechanisms that proceed in ALS. The 2D mapping and imaging capability is particularly important, offering a few micrometres lateral spatial resolution. Accordingly, there has been increasing interest in using FT-IR microspectroscopy for studies in medical research, including of neurological disorders.

## Materials and methods

The FT-IR measurements were performed for a sample of thoracic spinal cord. The specimens were taken during the autopsy of a 65-year old female patient deceased with amyotrophic lateral sclerosis. The duration of the disease was 13 months from ALS symptom onset to death. There were no other disorders in her medical history as well as positive family history of the ALS. She had been treated with the drug Riluzole since October 2001. The woman was diagnosed as having definite, sporadic amyotrophic lateral sclerosis (according to the El Escorial Criteria, 1998)<sup>10</sup> with bulbar onset. The clinical diagnosis was confirmed by electromyography examinations.

The histopathological examinations of spinal cord samples showed significant loss of motor neurons. Moreover, ubiquitin-positive inclusions were found in anterior horns in all ALS spinal cords. They were usually in the form of small cytoplasmic Bunina-body-like or skein-type deposits.

The specimens selected for investigation using FT-IR microspectroscopy were cryosectioned ( $-30^{\circ}\text{C}$ ) to a thickness of  $20\ \mu\text{m}$ . From each section one slice was stained with hematoxyline-eosin and the other one was used for measurements using FT-IR microspectroscopy. The slices for infrared analysis were mounted on ultra-pure, ultra-thin polymer AP1 (Moxtek) foil and then freeze-dried.

The FT-IR measurements were carried out at LURE (Orsay, France) on the Mirage SA5 synchrotron beamline. The conventional thermal (globar) source of IR was also used for large area mapping at low spatial resolution. The IR microspectroscopic maps were collected in transmission mode using an infrared microscope (NicPlan, Thermo Nicolet) coupled to a FT-IR spectrometer (Magma 550, Thermo-Nicolet). The IR microscope was equipped with a motorised sample stage (precision  $1\ \mu\text{m}$ ) and a liquid nitrogen cooled mercury cadmium telluride (MCT) detector. The analysis and maps generated were achieved using a projected area on the sample of  $18\ \mu\text{m} \times 18\ \mu\text{m}$  and a step size of  $10\ \mu\text{m}$ . Each spectrum was acquired from 100 accumulations at  $8\ \text{cm}^{-1}$  spectral resolution. Data acquisition and processing were performed using Omnic software (Thermo Nicolet).

## Results

The FT-IR spectroscopic analysis of the biomolecules was performed in the area of

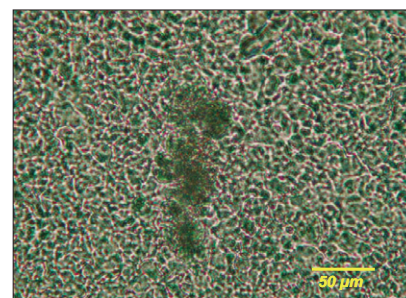


**Figure 1.** Visible image showing the area scanned by FT-IR microspectroscopy.

the ventral horn of spinal cord. The tissue area was mapped to generate two-dimensional images of the main biological molecules. The visible microscopic view of the scanned area of the ALS sample is shown in Figure 1. The infrared mapping was performed in the region containing the dark inclusion. The size of the observed inclusion was about  $50\ \mu\text{m} \times 100\ \mu\text{m}$ . The FT-IR absorption spectra collected in this area revealed specific vibrational bands not present in the spectra recorded outside the inclusion. In Figure 2, the comparison of the FT-IR spectra from the inclusion and its surrounding area are shown. The assignments of absorption peaks frequently observed in the FT-IR spectra of biological materials are reported in Table 1.<sup>11</sup> The spectrum of the unknown compound, resulting from the subtraction of the spectrum recorded from inside the inclusion minus the spectrum recorded

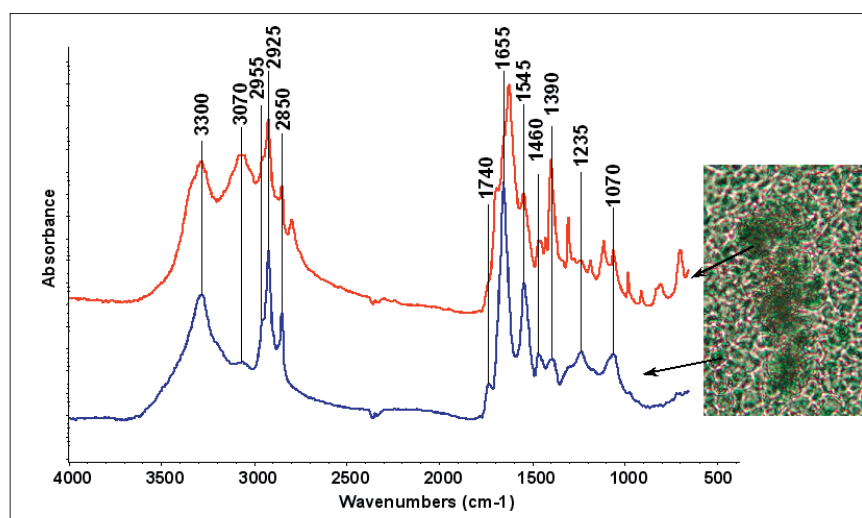


**Figure 2.** FT-IR spectra recorded from the inclusion (red spectrum) and outside of the inclusion (blue spectrum).

**Table 1.** Tentative assignments of the band frequencies typical for biological molecules.

Frequency (cm <sup>-1</sup> )	Assignment
3400–3200	OH str
~3300	N–H str (protein, amide A)
~3070	N–H str (protein, amide B)
~2955	CH <sub>3</sub> asym str (lipids)
~2925	CH <sub>2</sub> asym str (lipids)
~2850	CH <sub>2</sub> sym str (lipids)
1750–1720	C=O str (ester, lipids)
~1655	Amide I: CO str, CN str, NH bend (protein)
~1545	Amide II: NH bend, CN str (protein)
~1460	CH <sub>2</sub> sciss; CH <sub>3</sub> asym bend (lipids)
~1380	CH <sub>3</sub> sym bend (lipids)
~1300	Amide III: CN str, NH bend, CO str, O=C–N bend (protein)
1260–1220	PO <sub>2</sub> asym str (nucleic acids)
~1170	CO–O–C antisymmetric stretching (lipid)
~1085	PO <sub>2</sub> sym str (nucleic acids)

str: stretching; asym: antisymmetric; sym: symmetric; bend: bending; vib: vibration; sciss: scissoring

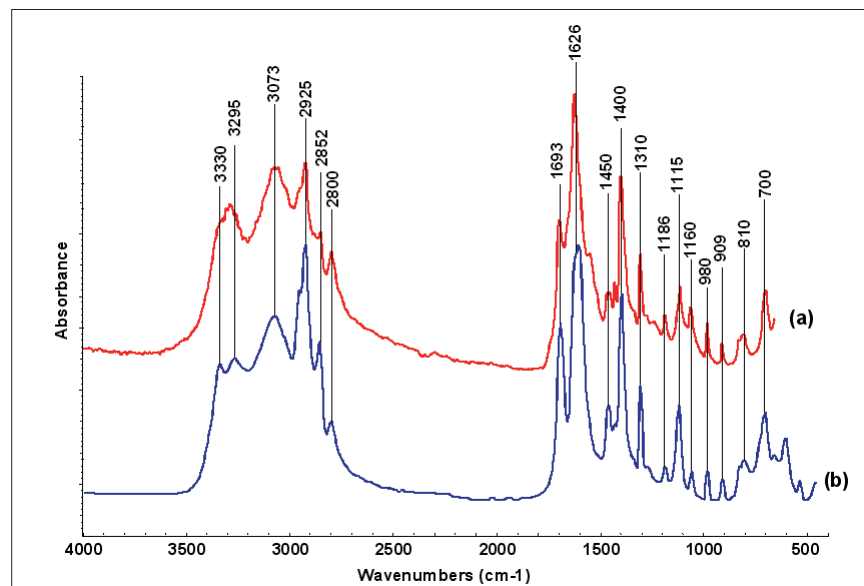


**Figure 3.** Red spectrum is a FT-IR difference spectrum generated from the two spectra shown in Figure 2. Blue spectrum is a database reference spectrum of creatine.

from outside the inclusion, was submitted to a database search, from which creatine was clearly identified (see Figure 3). The typical absorption bands of creatine are indicated in Figure 3. Taken into account the correlation between the number, position and relative intensity of the spectral

bands, the identification of the unknown compound as creatine is unambiguous.

Chemical images based on some characteristic absorption bands of creatine (2800 cm<sup>-1</sup>, 1400 cm<sup>-1</sup> and 1310 cm<sup>-1</sup>) are displayed in Figure 4. The shape of creatine deposit on the IR spectroscopy

generated maps correlates perfectly with the optical image of the dark inclusion in the tissue section. This indicates a co-localisation of creatine with the inclusion in the tissue section. As creatine is a critical component in maintaining cellular energy homeostasis, these findings may be interpreted as a mechanism of an impaired energy metabolism in the neuronal death cascade in ALS.

## Discussion

The obtained results clearly indicated the presence of creatine deposits in the ALS spinal cord tissue section. However, the occurrence of this relatively large deposit is unclear. Different kinds of inclusions, including Bunina bodies, large hyaline, Lewy-body-like inclusions, and ubiquitinated inclusions were found in histopathological slides in the case of ALS.<sup>4</sup> The creatine inclusions were not observed in these studies. Microcrystalline deposits of creatine were detected by Gallant *et al.* using infrared microspectroscopy in transgenic mice expressing doubly mutant (K670N/M671L and V717F) with advanced plaque pathology.<sup>12</sup> Relatively large creatine deposits were also found by this group in hippocampal sections from post-mortem Alzheimer diseased human brain.

Creatine is normally present in the human body and is a critical component in maintaining cellular energy homeostasis. Creatine kinase (CK) and its substrates creatine and phosphocreatine constitute an intricate cellular energy buffering and transport system connecting sites of energy production (mitochondria) with sites of energy consumption.<sup>13</sup> By reversible interconversion of creatine into phosphocreatine, CK builds up a large pool of rapidly diffusing phosphocreatine for temporal and spatial buffering of ATP levels. Thus, CK plays a particularly important role in tissues with large and fluctuating energy demands like muscle and brain, with the mitochondrial isoenzyme of CK being important for the energetics of oxidative tissue.<sup>14</sup>

There are a number of interrelated pathogenic mechanisms triggering molecular events that lead to neuronal death.<sup>15</sup> One putative mechanism reported to play a critical role in the pathogenesis and

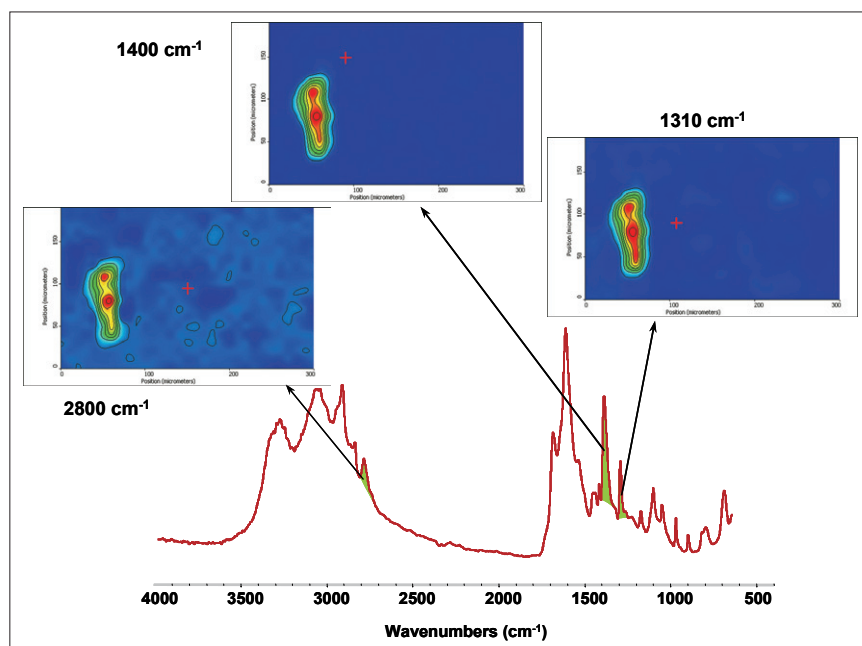


**Figure 4.** FT-IR spectroscopic images generated based on the relative absorption area intensities of bands at 2800, 1400 and 1310  $\text{cm}^{-1}$  from the difference spectrum shown in Figure 3.

progression of neurological diseases as a primary and/or secondary mechanism in the neuronal death cascade is impaired energy metabolism. This is due to abnormalities in the respiratory chain or altered superoxide dismutase, leading to generation of reactive oxygen species, a deteriorated energetic state and finally to necrotic and apoptotic cell death.<sup>16</sup> Mitochondrial dysfunction is one of the indicators of ischemia/reperfusion damage, as well as of many neuro-muscular dystrophies and neurodegenerative or other age-related disorders.<sup>16–19</sup> An aberrant cytosol/membrane partitioning of CK, as well as CK inactivation, were observed in amyotrophic lateral sclerosis (ALS).<sup>20</sup>

If reduced energy stores play a role in neuronal loss, then therapeutic strategies that buffer intracellular energy levels may prevent or impede the neurodegenerative process. The administration of creatine has been reported to be neuroprotective in a wide number of both acute and chronic experimental models of neurological disease, e.g. ALS.<sup>21</sup> Supportive to a role of the CK system in these disorders is the protective effect of creatine supplementation that has been observed in several studies, including animal models of amyotrophic lateral sclerosis.<sup>21</sup>

The results obtained with the use of FT-IR microspectroscopy may reflect the abnormalities in creatine-dependent reactions. Further studies into the connection between ALS and creatine deposits in central nervous system tissue are therefore warranted.

### Acknowledgements

This work was supported by the Ministry of Science and High Education (Warsaw, Poland) and the LURE experimental grant IM 017–03.

### References

1. M.T. Carri, A. Ferri, M. Cozzolino, L. Calabrese and G. Rotilio, *Brain Res. Bull.* **61**, 365–374 (2003).
2. B. Tomik, J. Chwiej, M. Szczerbowska-Boruchowska, M. Lankosz, S. Wójcik, D. Adamek, G. Falkenberg, S. Bohic, A. Simionovici, Z. Stegowski and A. Szczudlik, *Neurochem. Res.* **4**, 321–331 (2006).
3. C.A. Ross and M.A. Poirier, *Nat. Med.* **10**, 10–17 (2004).
4. D. Adamek, B. Tomik, A. Pichor, J. Kaluza and A. Szczudlik, *Folia Neuropathol.* **40**, 119–124 (2002).
5. C. Cappani, N. Taddei, S. Gabrielli, L. Messori, P. Orioli, F. Chiti, M. Stefani

- and G. Ramponi, *Cell. Mol. Life Sci.* **61**, 982–991 (2004).
6. M. Goedert and M.G. Spillantini, *Science* **314**, 777–781 (2006).
7. B. Stuart, *Modern infrared spectroscopy*. John Wiley & Sons, Chichester (1996).
8. D. Naumann, "FT-infrared and FT-Raman spectroscopy", in *Biomedical research: infrared and Raman spectroscopy of biological materials*, Ed by H.-U. Gremlich and B. Yan. Marcel Dekker, New York (2001).
9. D.M. Byler and H. Susi, *Biopolymers* **25**(3), 469–487 (1986).
10. B.R. Brooks, R.G. Miller, M. Swash and T.L. Munsat, *Amyotroph Lateral Scler. Other Motor Neuron Disord.* **1**(5), 293–299 (2000).
11. G. Socrates, *Infrared and Raman Characteristic Group Frequencies*, 3rd Edn. John Wiley & Sons, Chichester (2004).
12. M. Gallant, M. Rak, A. Szeghalmi, M.R. Del Bigio, D. Westaway, J. Yang, R. Julian and K.M. Gough, *J. Biol. Chem.* **281**(1), 5–8 (2006).
13. P. Klivenyi, R.J. Ferrante, R.T. Matthews, M.B. Bogdanov, A.M. Klein, O.A. Andreassen, G. Mueller, M. Wermer, R. Kaddurah-Daouk and M.F. Beal, *Nat. Med.* **5**(3), 347–350 (1999).
14. U. Schlattner, M. Tokarska-Schlattner and T. Wallimann, *Biochim. Biophys. Acta* **1762**(2), 164–180 (2006).
15. A.M. Klein and R.J. Ferrante, *Subcell. Biochem.* **46**, 205–243 (2007).
16. S. Raha and B.H. Robinson, *Trends Biochem. Sci.* **25**, 502–508 (2000).
17. M.F. Beal, *Trends Neurosci.* **23**, 298–304 (2000).
18. R.S. Sohal and R. Weindruch, *Science* **273**, 59–63 (1996).
19. M.A. Tarnopolsky and M.F. Beal, *Ann. Neurol.* **49**, 561–574 (2001).
20. S. Wendt, A. Dedeoglu, O. Speer, T. Wallimann, M.F. Beal and O.A. Andreassen, *Free Radical Biol. Med.* **32**, 920–926 (2002).
21. P. Klivenyi, R.J. Ferrante, R.T. Matthews, M.B. Bogdanov, A.M. Klein, O.A. Andreassen, G. Mueller, M. Wermer, R. Kaddurah-Daouk and M.F. Beal, *Nat. Med.* **5**, 347–350 (1999).